

S. THANASANVORAKUN¹, A. PHURUANGRAT², S. THONGTEM^{3,4*}, S. JAITA⁵,
T. THONGTEM^{3,6}, P. DUMRONGROJTHANATH^{7*}

MICROWAVE-ASSISTED SYNTHESIS OF Nd-DOPED BiOBr MICROFLOWERS AND PHOTODEGRADATION OF RHODAMINE B MOLECULES

0-3% Nd-doped BiOBr microflowers were synthesized by a one-step microwave-assisted method. Phase, morphology and optical property of Nd-doped BiOBr samples were characterized by XRD, SEM, TEM, XPS and photoluminescence (PL) spectroscopy. The samples were investigated for the degradation of rhodamine B (RhB) under UV-visible radiation of a 35 W xenon lamp for 60 min. The results showed that the degradation efficiencies of Nd doped BiOBr samples were higher than that of the un-doped BiOBr. The 2%Nd-doped BiOBr sample shows the highest photocatalytic activity of 98% and has a good reusability and photostability within three cycles. During the photocatalysis of 2% Nd doped BiOBr, the main active species in degrading of RhB were superoxide radical ($\cdot\text{O}_2^-$) and hole (h^+).

Keywords: Nd-doped BiOBr microflowers; Microwave-assisted method; Photocatalysis; Spectroscopy

1. Introduction

Nowadays the increase of industries has been led to cause environmental and human health problems which can lead to increase organic pollutants in wastewater [1,2]. Organic dyes from textile production such as rhodamine B, methylene blue and methyl orange are hazardous contaminants which can destroy ecological environment of water reservoirs [3-5]. Several methods have been used to remove organic dye contaminants containing in wastewater and photocatalysis as an interesting method is used to remove the organic dyes because the process is non-toxic, cost effective and very high efficiency [6-8].

Among different photocatalysts, Bi-based oxide semiconductor such as bismuthoxybromide (BiOBr) is very interesting material because it has good photocatalytic property, non-toxic property to the environment and high chemical stability [1,9,10]. BiOBr has suitable band gap energy of 2.6-2.8 eV, therefore, it is able to be excited by UV-visible light [11,12]. Although BiOBr has high advantage for photocatalysis, it is limited by the recombination of photo-induced electron-hole pairs. To solve

this problem, rare earth elements have optimistic electronic property, improvement of spectrum absorption and enhance quantum efficiency [5, 11-13]. Semiconductors doped with rare earth elements can lead to reduce electron-hole pair recombination because the incompletely occupied 4f and empty 5d orbitals play the role in trapping electrons and holes, and interacting of f-orbitals of rare earth elements and semiconductors. In particular, Nd-doped semiconductor has been demonstrated as a good photocatalyst because of its ability to harvest visible light and the creation of oxygen vacancy [14-18]. BiOBr materials with different shapes and sizes such as nanosheets [9,11], nanoplates [13], nanoparticles [19], nanobelts [20], and 3D microflowers [8,21,22] have been synthesized. Among them, the 3D microstructure has excellent photocatalytic performance due to its high specific surface area, more pore volume and effective charge-separation [8,21,22].

In this work, Nd-doped BiOBr microflowers were synthesized by microwave-assisted method. The as-prepared products were characterized by different methods. Photocatalytic activity was investigated through the degradation of rhodamine B illuminated by UV-visible radiation.

¹ RAJAMANGALA UNIVERSITY OF TECHNOLOGY LANNA, FACULTY OF SCIENCE AND AGRICULTURAL TECHNOLOGY, CHIANG MAI 53000, THAILAND

² PRINCE OF SONGKLA UNIVERSITY, FACULTY OF SCIENCE, DIVISION OF PHYSICAL SCIENCE, HAT YAI, SONGKHLA 90112, THAILAND

³ CHIANG MAI UNIVERSITY, FACULTY OF SCIENCE, MATERIALS SCIENCE RESEARCH CENTER, CHIANG MAI 50200, THAILAND

⁴ CHIANG MAI UNIVERSITY, FACULTY OF SCIENCE, DEPARTMENT OF PHYSICS AND MATERIALS SCIENCE, CHIANG MAI 50200, THAILAND

⁵ RAJAMANGALA UNIVERSITY OF TECHNOLOGY LANNA, FACULTY OF SCIENCE AND AGRICULTURE TECHNOLOGY, CHIANG RAI 57120, THAILAND

⁶ CHIANG MAI UNIVERSITY, FACULTY OF SCIENCE, DEPARTMENT OF CHEMISTRY, CHIANG MAI 50200, THAILAND

⁷ RAJAMANGALA UNIVERSITY OF TECHNOLOGY LANNA, FACULTY OF SCIENCE AND AGRICULTURAL TECHNOLOGY, NAN 55000, THAILAND

* Corresponding authors: d.phattranit@gmail.com, schthongtem@yahoo.com



2. Experimental details

Typically, 0.006 mol $\text{Bi}(\text{NO}_3)_3 \cdot 5\text{H}_2\text{O}$ and 0-5 mol% $\text{Nd}(\text{NO}_3)_3 \cdot 6\text{H}_2\text{O}$ were dissolved in 20 ml 3M HNO_3 labelled as a solution A. In addition, 0.006 mol KBr was dissolved in 80 ml DI water which was dropped into the solution A under continued stirring. The stirred solution was adjusted the pH to 8 by NH_4OH and stirred for 30 min. The mixed solution was irradiated by 2.45 GHz microwave at 300 W for 1h. In the end, the as-prepared products were separated by filtering, washed with DI water and absolute ethanol, and dried at 70°C for 24 h for further characterization.

An X-ray diffractometer (XRD, Rigaku SmartLab) was used to analyse crystallinity and purity of the as-prepared product. Morphology and microstructure of the as-prepared product were characterized by a Field Emission Scanning Electron Microscope (FE-SEM, JEOL JSM-6335F) and a Transmission Electron Microscope (TEM, JEOL JEM-2010). XPS analysis was obtained by an X-ray photoelectron spectrometer (Kratos Axis Ultra DLD). The PL spectra were analysed by a Jasco FP8500 spectrofluorometer at an excitation wavelength of 439 nm.

Photocatalytic activities of the samples were investigated through the degradation of Rhodamine B (RhB) solution irradiated with a 35 W xenon lamp. First, 200 mg of the as-prepared sample as a photocatalyst was dispersed in 200 ml of 5×10^{-5} M RhB solution and followed by stirring with a magnetic stirrer for 30 min in the dark for an adsorption-desorption equilibrium before irradiation. Second, the xenon lamp was turned on to illuminate the solution system. In the end, 5 ml of the solution was sampled every 10 min interval and followed by centrifugation to remove the solid residue. The RhB solution without the solid residue was analysed at the peak absorption of 554 nm by a Hitachi U-2900 UV-visible spectrophotometer. The degradation efficiency (%) was calculated by the following.

$$\text{Degradation efficiency (\%)} = \frac{C_0 - C_t}{C_0} \times 100 \quad (1)$$

C_0 is the initial concentration of RhB and C_t is the concentration of RhB after the elapsed time (t).

3. Results and discussion

XRD patterns of 0-3%Nd-doped BiOBr are presented in Fig. 1. For the product without being doped with Nd, all diffraction peaks correspond to tetragonal BiOBr with lattice parameter of $a = b = 3.9233 \text{ \AA}$, $c = 8.1050 \text{ \AA}$ (JCPDS card No. 01-078-0348) [23]. No impurities such as Nd_2O_3 and Bi_2O_3 were detected and the product was very pure. The peaks of 1, 2 and 3%Nd-doped BiOBr products were slightly shifted to higher angles with respect to those of the un-doped BiOBr. It is ascribable to the ionic size difference. The ionic radius of Nd^{3+} (0.098 nm) is shorter than the ionic radius of Bi^{3+} (0.103 nm). Clearly, Nd^{3+} was successfully substituted for Bi^{3+} of the BiOBr lattice. Moreover, the diffraction peaks of the as-prepared products were lowered

and broader with the increase of Nd^{3+} content because atomic arrangement of BiOBr crystal was de-organized [15,16, 24-26].

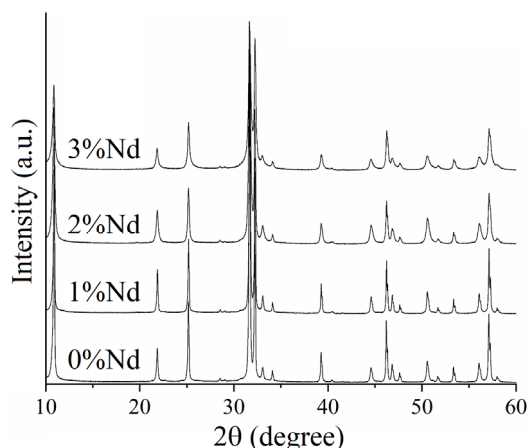


Fig. 1. XRD patterns of 0-3% Nd-doped BiOBr products

The surface chemical composition and oxidation state of 2%Nd-doped BiOBr were characterized by an XPS analyser (Fig. 2). The high-resolution Bi 4f shows two strong peaks at 159.1 eV and 164.4 eV corresponding to $\text{Bi } 4f_{7/2}$ and $\text{Bi } 4f_{5/2}$ chemical states of Bi^{3+} containing in the product. The binding energy of O 1s was de-convoluted into three peaks. Those at 530.5 eV and 531.7 eV are attributed to the Bi-O bond of the BiOBr product. The peak at 533.0 eV is caused by oxygen of hydroxyl group or H_2O on the product surface. The Br 3d was disintegrated into two peaks at 68.1 eV and 69.2 eV which correspond to $\text{Br } 3d_{5/2}$ and $\text{Br } 3d_{3/2}$ binding energies of BiOBr. Two peaks at 983.3 eV and 1006.1 eV are attributed to $\text{Nd } 3d_{5/2}$ and $\text{Nd } 3d_{3/2}$ orbitals, respectively. They should be noted that Nd^{3+} belongs to the product [27-31]. The XRD and XPS results indicate that Nd element was successfully incorporated into the BiOBr lattice by the one step microwave-assisted method.

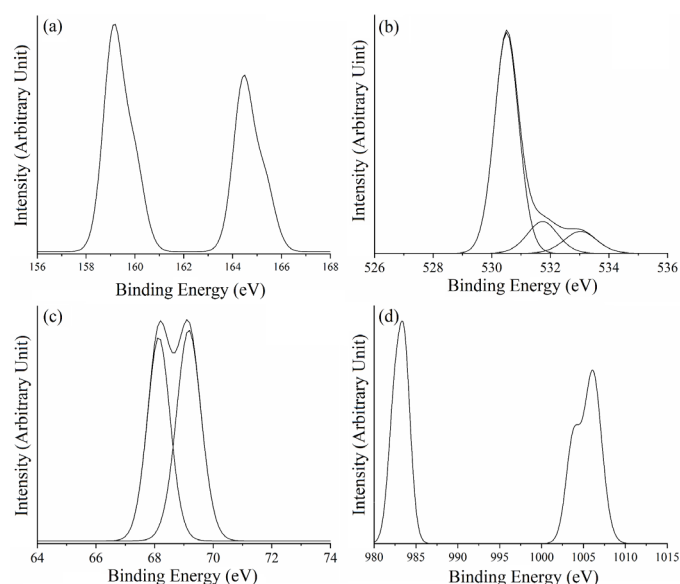


Fig. 2. XPS spectra of (a) Bi 4f, (b) O 1s, (c) Br 3d and (d) Nd 3d of 2% Nd-doped BiOBr

The morphology of 0-3%Nd-doped BiOBr samples was investigated by SEM and TEM. The SEM image of Fig. 3a shows that the product appears as flowers constructed by thin nanoplates with an average diameter of 4-5 nm. SEM images of 1-3% Nd-doped BiOBr samples (Fig. 3b-d) present microflowers with no significant difference in morphology as compared with the un-doped sample. They should be noted that Nd dopant has only a slight influence on the morphology. These microflowers were composed of porous structure of nanoplate petals that can lead to enhance the harvest of solar energy and absorption of photon by diffraction and reflection in the photocatalytic interface and the photocatalytic activity of the material. The surface of a photocatalytic semiconductor can play the role in the photocatalytic activity. Rough surface has high specific surface area and abundant transport paths for organic molecules which can lead to enhance the photocatalytic activity [5,22,32-33]. In addition, the TEM images of pure BiOBr and 2% Nd-doped BiOBr samples (Fig. 4a and 4c) show that they were composed

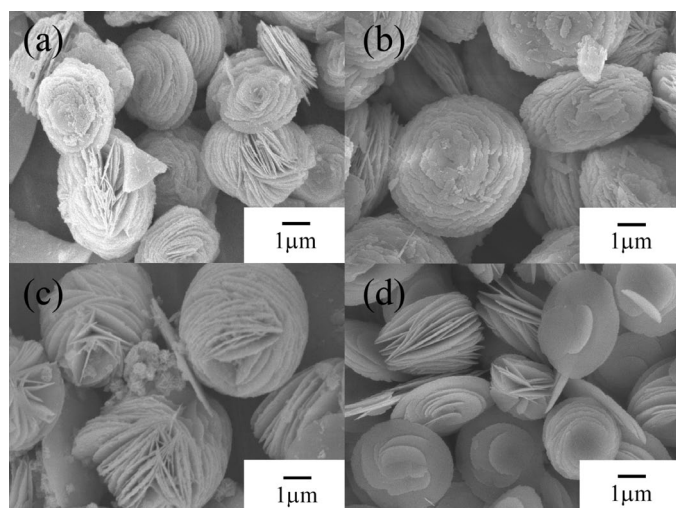


Fig. 3. SEM images of (a) pure BiOBr, (b) 1% Nd-doped BiOBr, (c) 2% Nd-doped BiOBr, (d) 3% Nd-doped BiOBr samples prepared by microwave-assisted method

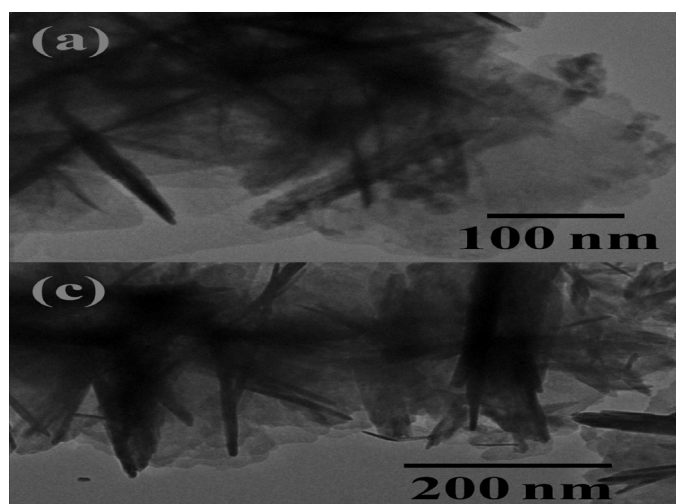


Fig. 4. TEM and HRTEM images of (a, b) pure BiOBr and (c, d) 2% Nd-doped BiOBr

of microflowers constructed by nanoplates with a thickness of 15-30 nm. HRTEM images of un-doped BiOBr and 2%Nd-doped BiOBr (Fig. 4b and 4d) show lattice fringes with inter-planar spaces of 0.351 nm and 0.354 nm corresponding to the (101) plane of tetragonal BiOBr. The lattice fringe was enlarged by the introduction of Nd dopant into the BiOBr matrix. The HRTEM and XRD analyses are in correspondence. The ionic radius of Bi^{3+} is larger than that of Nd^{3+} and the lattice of BiOBr was reduced by the substitution of Nd^{3+} for Bi^{3+} of BiOBr lattice [19,34-35].

The photocatalytic performance of 0-3%Nd-doped BiOBr (Fig. 5a) was evaluated through the degradation of rhodamine B (RhB) irradiated by a xenon lamp. The un-doped BiOBr shows 45% degradation within 60 min. The photocatalytic performance of BiOBr was increased to the highest of 98% when 2% Nd was doped. This indicates that Nd dopant played the role in the photocatalytic activity of BiOBr because its band gap was narrowed. Thus, the separation efficiency of the photo-induced electron-hole pairs and the photocatalytic efficiency for the degradation of RhB were enhanced [15,17,29]. Upon further increasing the amount of Nd to 3%, the degradation efficiency was lessened to 80% because the extra Nd played the role in the recombination center. The excessive Nd on the surface of the BiOBr catalyst can lead to reduce the distance of the capture point and the recombination rate of electron-hole pairs was increased [5,8,14,25]. The kinetics of RhB degradation was investigated by pseudo-first-order kinetic reaction. The first-order kinetics constant (k) can be calculated by the Langmuir Hinshelwood kinetic model through the equation $\ln(C_0/C_t) = kt$, where k is the rate constant, and C_0 and C_t are the RhB concentration at the time 0 and t [24, 36-38]. The linear fitted plot of all products (Fig. 5b) shows that the 2%Nd-doped BiOBr has the highest rate for the degradation of RhB of 0.0556 min^{-1} .

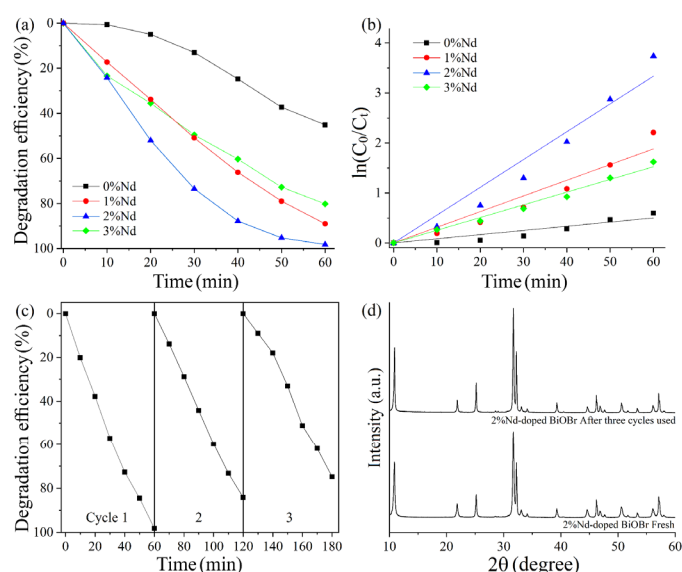


Fig. 5. (a) Degradation efficiency and (b) pseudo-first-order plot for photocatalysis of 0-3% Nd-doped BiOBr samples, (c) three cycled tests of 2% Nd-doped BiOBr for RhB degradation, and (d) XRD patterns of 2% Nd-doped BiOBr sample before and after three recycles of photocatalysis

Stability and reusability are the important factors of photocatalysts. To evaluate these factors, 2%Nd-doped BiOBr photocatalyst was carried out for photocatalysis under the same condition for three cycles as the results shown in Fig. 5c. At the end of the 3rd cycle, the photodegradation efficiency of 2%Nd-doped BiOBr photocatalyst was 71%. According to Fig. 5d, XRD pattern of the reused catalyst was very similar to that of the as-prepared sample with no impurity detection. Thus, the 2%Nd-doped BiOBr photocatalyst has a good stability and is a realistic use for wastewater treatment.

Photocatalytic activity of the as-prepared product is related with the recombination rate of photo-induced electron-hole pairs containing in the semiconductor. To investigate the recombination rate, the un-doped BiOBr and 2%Nd-doped BiOBr were characterized by photoluminescence (PL) spectroscopy as the results shown in Fig. 6a. Their emission peaks are at the same wavelength of 439 nm. In this research, the PL intensity of 2%Nd-doped BiOBr is lower than that of the un-doped sample. PL intensity is related with the charge separation of the semiconductor. Low PL intensity denotes to high separation efficiency and low recombination rate which lead to high photocatalytic performance [4,22,36]. The 2% Nd-doped BiOBr sample has photocatalytic performance better than the un-doped one. Thus, Nd dopant played the role in reducing the recombination rate and enhancing the photocatalytic performance of the sample under visible radiation.

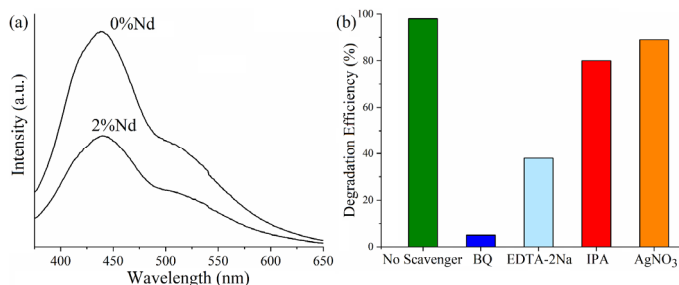


Fig. 6. (a) Emission spectra of 0 and 2% Nd-doped BiOBr samples and (b) effect of different scavengers on the degradation of RhB photocatalyzed by 2% Nd-doped BiOBr

To investigate the active species used for the photodegradation process of 2% Nd-doped BiOBr, different scavengers were also added to the photocatalytic solution system. Among them, p-benzoquinone (BQ), ethylenediaminetetraacetic acid disodium salts (EDTA-2Na), isopropanol (IPA) and silver nitrate (AgNO₃) were used to probe superoxide radical ($\bullet\text{O}_2^-$), active hole (h^+), hydroxyl radical ($\bullet\text{OH}$) and photo-excited electron (e^-), respectively. According to the results shown in Fig. 6b, the degradation rate of RhB solutions containing BQ, EDTA-2Na, IPA and AgNO₃ are 5%, 38%, 80% and 89%, respectively. Thus, $\bullet\text{O}_2^-$ and h^+ were the important active species that played the role in dramatic degradation of RhB. On the other hand, the removal rate of RhB was slightly decreased when IPA and AgNO₃ were added. These results imply that $\bullet\text{OH}$ and e^- were the auxiliary active species in the photocatalytic process.

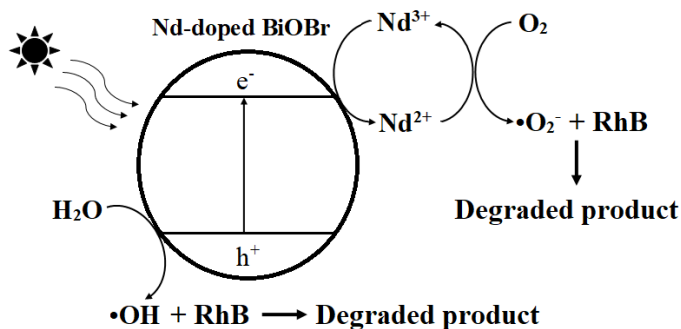
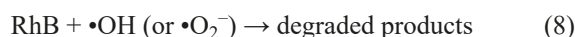
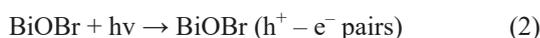


Fig. 7. A schematic diagram for photocatalysis of Nd-doped BiOBr in degrading RhB

Based on the above, photocatalysis mechanism of Nd-doped BiOBr (Fig. 7) is proposed according to the following.



When the Nd-doped BiOBr photocatalyst was activated by UV-visible light, electrons at the valence band (VB) were excited to the conduction band (CB). Thus, $e^- - h^+$ pairs resided in the CB and VB of BiOBr. Nd³⁺ ions can play the role in trapping the excited electrons and enhancing the separation of electrons and holes. Upon releasing the electrons, the Nd²⁺ ions were transformed into Nd³⁺ ions and the released electrons reacted with adsorbed O₂ to produce $\bullet\text{O}_2^-$. Concurrently, the photo-induced h^+ reacted with water molecules and hydroxyl ions to produce $\bullet\text{OH}$. Further, these strong oxidizing agents reacted with RhB molecules and changed the RhB into smaller molecules [3,8,14,24,26,34,39]. The separation of charge carriers of BiOBr was enhanced and its photocatalytic activity was improved. Thus, the Nd-doped BiOBr product is a promising photocatalyst used for wastewater treatment.

4. Conclusions

0-3% Nd-doped BiOBr products synthesized by microwave-assisted method were investigated for photocatalysis through the degradation of Rhodamine B under UV-visible radiation within 60 min. According to XRD analysis, all the products were tetragonal structure BiOBr. SEM and TEM analyses showed that the products were microflowers constructed by nanoplates. The photocatalytic efficiency of 2%Nd-doped BiOBr was the highest at 98%. The Nd dopant can play the role in improving the photocatalytic performance because of the enhancement of

electron-hole pairs separation and the reduction of electron-hole recombination. In this research, Nd-doped BiOBr is a good photocatalytic material that can be used to degrade organic molecules containing in wastewater.

Acknowledgments

We wish to thank Center of Excellence in Materials Science and Technology, Chiang Mai University for financial support under the administration of Materials Science Research Center, Faculty of Science, Chiang Mai University (CMU), and Rajamangala University of Technology Lanna through a general support.

REFERENCES

- [1] S. Fu, W. Yuan, X. Liu, Y. Yan, H. Liu, L. Li, F. Zhao, J. Zhou, A novel 0D/2D WS₂/BiOBr Heterostructure with Rich Oxygen Vacancies for Enhanced Broad-spectrum Photocatalytic Performance. *J. Colloid Interface Sci.* **569**, 150-163 (2020). DOI: <https://doi.org/10.1016/j.jcis.2020.02.077>
- [2] B. Zhang, M. Zhang, L. Zhang, P.A. Bingham, M. Tanaka, W. Li, S. Kubuki, BiOBr/MoS₂ Catalyst as Heterogenous Peroxymonosulfate Activator Toward Organic Pollutant Removal: Energy Band Alignment and Mechanism Insight. *J. Colloid Interface Sci.* **594**, 635-649 (2021). DOI: <https://doi.org/10.1016/j.jcis.2021.03.066>
- [3] J. Ebrahimian, M. Mohsennia, M. Khayatkashani, Green Synthesis and Characterization of Ud-SnO₂-ZnO using *Urtica Dioica* Leaf Extract: A Nanocomposite Photocatalyst for Degradation of Rhodamine B Dye. *Res. Chem. Intermed.* **47**, 4789-4802 (2021). DOI: <https://doi.org/10.1007/s11164-021-04546-z>
- [4] T.M. Budnyak, J. Onwumere, I.V. Pylypchuk, A. Jaworski, J. Chen, A. Rokicińska, M.E. Lindström, P. Kuśtrowski, O. Sevastyanova, A. Slabon, LignoPhot: Conversion of Hydrolysis Lignin into the Photoactive Hybrid lignin/Bi₄O₅Br₂/BiOBr Composite for Simultaneous Dyes Oxidation and Co²⁺ and Ni²⁺ Recycling. *Chemosphere* **279**, 130538 (2021). DOI: <https://doi.org/10.1016/j.chemosphere.2021.130538>
- [5] C. Li, B. Wang, F. Zhang, N. Song, G. Liu, C. Wang, S. Zhong, Performance of Ag/BiOBr/GO Composite Photocatalyst for Visible-light-driven Dye Pollutants Degradation. *J. Mater. Res. Technol.* **9**, 610-621 (2020). DOI: <https://doi.org/10.1016/j.jmrt.2019.11.001>
- [6] J. Qu, Y. Du, Y. Feng, J. Wang, B. He, M. Du, Y. Liu, N. Jiang, Visible-light-responsive K-doped g-C₃N₄/BiOBr Hybrid Photocatalyst with Highly Efficient Degradation of Rhodamine B and Tetracycline. *Mater. Sci. Semicond. Process* **112**, 105023 (2020). DOI: <https://doi.org/10.1016/j.mssp.2020.105023>
- [7] S. Liang, D. Zhang, X. Yao, R. Han, Q. Zhang, C. Jin, X. Pu, Y. Geng, Deposition-Precipitation Synthesis of Yb³⁺/Er³⁺ codoped BiOBr/AgBr Heterojunction Photocatalysts with Enhanced Photocatalytic Activity under Vis/NIR Light Irradiation. *Sep. Purif. Technol.* **238**, 116450 (2020). DOI: <https://doi.org/10.1016/j.seppur.2019.116450>
- [8] S. Yin, W. Fan, J. Di, T. Wu, J. Yan, M. He, J. Xia, H. Li, La³⁺ doped BiOBr Microsphere with Enhanced Visible Light Photocatalytic Activities. *Colloids Surf. A* **513**, 160-167 (2017). DOI: <http://dx.doi.org/doi:10.1016/j.colsurfa.2016.10.012>
- [9] D. Wu, S. Yue, W. Wang, T. An, G. Li, H. Yin, Y. Huijun, Z. Po, K. Wong, Boron doped BiOBr Nanosheets with Enhanced Photocatalytic Inactivation of *Escherichia coli*. *Appl. Catal. B* **192**, 35-45 (2016). DOI: <http://dx.doi.org/doi:10.1016/j.apcatb.2016.03.046>
- [10] Q. Jiang, M. Ji, R. Chen, Y. Zhang, K. Li, C. Meng, Z. Chen, H. Li, J. Xia, Ionic Liquid Induced Mechanochemical Synthesis of BiOBr Ultrathin Nanosheets at Ambient Temperature with Superior Visible-light-driven Photocatalysis. *J. Colloid Interface Sci.* **574**, 131-139 (2020). DOI: <https://doi.org/10.1016/j.jcis.2020.04.018>
- [11] W. Huang, X. Hua, Y. Zhao, K. Li, L. Tang, M. Zhou, Z. Cai, Enhancement of Visible-light-driven Photocatalytic Performance of BiOBr Nanosheets by Co²⁺ Doping. *J. Mater. Sci.: Mater. Electron.* **30**, 14967-14976 (2019). DOI: <https://doi.org/10.1007/s10854-019-01869-x>
- [12] M. Zhou, W. Huang, Y. Zhao, Z. Jin, X. Hua, K. Li, L. Tang, Z. Cai, 2D g-C₃N₄/BiOBr Heterojunctions with Enhanced Visible Light Photocatalytic Activity. *J. Nanopart. Res.* **22**, 13 (2020). DOI: <https://doi.org/10.1007/s11051-019-4739-3>
- [13] M. Hu, A. Yana, X. Wang, F. Huang, Q. Cui, F. Li, J. Huang, Hydrothermal Method to Prepare Ce-doped BiOBr Nanoplates with Enhanced Carrier Transfer and Photocatalytic Activity. *Mater. Res. Bull.* **116**, 89-97 (2019). DOI: <https://doi.org/10.1016/j.materresbull.2019.04.019>
- [14] J. Du, X. Gu, Q. Wu, J. Liu, H. Guo, J. Zou, Hydrophilic and Photocatalytic Activities of Nd-doped Titanium Dioxide Thin Films. *Trans. Nonferrous Met. Soc. China.* **25**, 2601-2607 (2015). DOI: <https://doi.org/10.1016/j.jphotochem.2021.113334>
- [15] Y. Hanifehpour, N. Hamnabard, B. Khomami, S.W. Joo, B.K. Min, J.H. Jung, A Novel Visible-light Nd-doped CdTe Photocatalyst for Degradation of Reactive Red 43: Synthesis, Characterization, and Photocatalytic Properties. *J. Rare Earths.* **34**, 45-54 (2016). DOI: [10.1016/S1002-0721\(14\)60576-7](https://doi.org/10.1016/S1002-0721(14)60576-7)
- [16] V. Rajendran, R. Mekala, Effect of Pure and REM: (Nd, Ce)-doped Dy₂O₃ NPs via Hydrothermal Method and Their Magnetic, Optical, Electrochemical, Antibacterial and Photocatalytic Activities. *J. Alloys Compd.* **741**, 1055-1069 (2018). DOI: <https://doi.org/10.1016/j.jallcom.2018.01.086>
- [17] U. Alam, T.A. Shah, A. Khan, M. Muneer, One-pot Ultrasonic Assisted Sol-gel Synthesis of Spindle-like Nd and V Codoped ZnO for Efficient Photocatalytic Degradation of Organic Pollutants. *Sep. Purif. Technol.* **212**, 427-437 (2018). DOI: <https://doi.org/10.1016/j.seppur.2018.11.048>
- [18] T. Cadenbach, P. Santillan, A. Lucia Morales, M.J. Benitez, F. Moncada, L. Lascano, C. Costa-Vera, V. Ochoa-Herrera, K. Vizuete, A. Debut, Synthesis of Doped and Undoped Bi_{1-x}M_xFeO₃ Porous Networks (M = La, Gd, Nd; x = 0, 0.03, 0.05, 0.10) with Enhanced Visible-light Photocatalytic Activity. *J. Photochem. Photobiol. A* **416**, 113334 (2021). DOI: <https://doi.org/10.1016/j.jphotochem.2021.113334>

- [19] J. Henle, P. Simon, A. Frenzel, S. Scholz, S. Kaskel, Nanosized BiOX (X Cl, Br, I) Particles Synthesized in Reverse Microemulsions. *Chem. Mater.* **19**, 366-373 (2007). DOI: <https://doi.org/10.1021/cm061671k>
- [20] H. Deng, J. Wang, Q. Peng, X. Wang, Y. Li, Controlled Hydrothermal Synthesis of Bismuth Oxyhalide Nanobelts and Nanotubes. *Chem. Eur. J.* **11**, 6519-6524 (2005). DOI: <https://doi.org/10.1002/chem.200500540>
- [21] J. Zhang, F. Shi, J. Lin, D. Chen, J. Gao, Z. Huang, X. Ding, C. Tang, Self-Assembled 3-D Architectures of BiOBr as a Visible Light-Driven Photocatalyst. *Chem. Mater.* **20**, 2937-2941 (2008). DOI: <https://doi.org/10.1002/chem.200500540>
- [22] L. Lin, M. Huang, L. Long, Z. Sun, W. Zheng, D. Chen, Fabrication of a Three-dimensional BiOBr/BiOI Photocatalyst with Enhanced Visible Light Photocatalytic Performance. *Ceram. Int.* **40**, 11493-11501 (2014). DOI: <http://dx.doi.org/10.1016/j.ceramint.2014.03.039>
- [23] Powder Diffract. File, JCPDS-ICDD, 12 Campus Blvd., Newtown Square, PA 19073-3273, U.S.A. (2001).
- [24] P. Dumrongrojthanath, T. Thongtem, A. Phuruangrat, S. Thongtem, Glycothermal Synthesis of Dy-doped Bi₂MoO₆ Nanoplates and Their Photocatalytic Performance. *Res. Chem. Intermed.* **42**, 5087-5097 (2016). DOI: <https://doi.org/10.1007/s11164-015-2346-1>
- [25] M. He, W. Li, J. Xia, L. Xu, J. Di, H. Xu, S. Yin, H. Li, M. Li, The Enhanced Visible Light Photocatalytic Activity of Yttrium-doped BiOBr Synthesized via a Reactable Ionic Liquid. *Appl. Surf. Sci.* **331**, 170-178 (2015). DOI: <http://dx.doi.org/doi:10.1016/j.apsusc.2014.12.141>
- [26] J. Zhou, J. Zhou, Z. Hu, Luo Wang, Enhancement of Adsorption and Visible Light Photocatalytic Activity of the Zn²⁺-doped BiOBr/PVP Modified Microspheres for RhB. *Mater. Sci. Semicond. Process.* **90**, 112-119 (2019). DOI: <https://doi.org/10.1016/j.mssp.2018.10.012>
- [27] Y. Wang, J. He, Y. Zhu, H. Zhang, C. Yang, K. Wang, S.C. Wu, Y.L. Chueh, W. Jiang, Hierarchical Bi-doped BiOBr Microspheres Assembled from Nanosheets with (001) Facet Exposed via Crystal Facet Engineering Toward Highly Efficient Visible Light Photocatalysis. *Appl. Surf. Sci.* **514**, 145927 (2020). DOI: <https://doi.org/10.1016/j.apsusc.2020.145927>
- [28] Y. Yao, M. Sun, X. Yuan, Y. Zhu, X. Lin, S. Anandan, One-step Hydrothermal Synthesis of N/Ti³⁺ Co-doping Multiphase TiO₂/BiOBr Heterojunctions Towards Enhanced Sonocatalytic Performance. *Ultrason. Sonochem.* **49**, 69-78 (2018). DOI: <https://doi.org/10.1016/j.ultsonch.2018.07.025>
- [29] J.C. Sin, C.A. Lim, S.M. Lam, H. Zeng, H. Lin, H. Li, A.R. Mohamed, Fabrication of Novel Visible Light-driven Nd-doped BiOBr Nanosheets with Enhanced Photocatalytic Performance for Palm Oil Mill Effluent Degradation and Escherichia Coli Inactivation. *J. Phys. Chem. Solids* **140**, 109382 (2020). DOI: <https://doi.org/10.1016/j.jpcs.2020.109382>
- [30] A. Chachvalvutikul, J. Jakmune, S. Thongtem, S. Kittiwachana, S. Kaowphong, Novel FeVO₄/Bi₇O₉I₃ Nanocomposite with Enhanced Photocatalytic Dye Degradation and Photoelectrochemical Properties. *Appl. Surf. Sci.* **475**, 175-184 (2019). DOI: <https://doi.org/10.1016/j.apsusc.2018.12.214>
- [31] X. Chen, X. Zhang, Y.H. Li, M.Y. Qi, J.Y. Li, Z.R. Tang, Z. Zhou, Y.J. Xu, Transition Metal Doping BiOBr Nanosheets with Oxygen Vacancy and Exposed {102} Facets for Visible Light Nitrogen Fixation. *Appl. Catal. B* **281**, 119516 (2021). DOI: <https://doi.org/10.1016/j.apcatb.2020.119516>
- [32] Y. Ling, Y. Dai, Direct Z-scheme Hierarchical WO₃/BiOBr with Enhanced Photocatalytic Degradation Performance Under Visible Light. *Appl. Surf. Sci.* **509**, 145201 (2020). DOI: <https://doi.org/10.1016/j.apsusc.2019.145201>
- [33] D. Gao, L. Wang, Q. Wang, Z. Qi, Y. Jia, C. Wang, Big-leaf Hydrangea-like Bi₂S₃-BiOBr Sensitized TiO₂ Nanotube Arrays with Enhanced Photoelectrocatalytic Performance. *Spectrochim. Acta, Part A* **229**, 117936 (2020). DOI: <https://doi.org/10.1016/j.saa.2019.117936>
- [34] W. Jiao, Y. Xie, F. He, K. Wang, Y. Ling, Y. Hu, J. Wang, H. Ye, J. Wu, Y. Hou, A Visible Light-response Flower-like La-doped BiOBr Nanosheets with Enhanced Performance for Photoreducing CO₂ to CH₃OH. *Chem. Eng. J.* **418**, 129286 (2021). DOI: <https://doi.org/10.1016/j.cej.2021.129286>
- [35] Q. Fan, X. Chen, F. Chen, J. Tian, C. Yu, C. Liao, Regulating the Stability and Bandgap Structure of BiOBr During Thermotransformation via La Doping. *Appl. Surf. Sci.* **481**, 564-575 (2019). DOI: <https://doi.org/10.1016/j.apsusc.2019.03.138>
- [36] L. Wang, X. Min, X. Sui, J. Chen, Y. Wang, Facile Construction of Novel BiOBr/Bi₁₂O₁₇C₁₂ Heterojunction Composites with Enhanced Photocatalytic Performance. *J. Colloid Interface Sci.* **560**, 21-33 (2020). DOI: <https://doi.org/10.1016/j.jcis.2019.10.048>
- [37] A. Tenczek-Zajac, J. Banaś, K. Świerczek, K. Zazakowny, M. Radecka, Photosensitization of TiO₂ P25 with CdS Nanoparticles for Photocatalytic Applications. *Arch. Metall. Mater.* **62** (2), 841-849 (2017). DOI: <https://doi.org/10.1515/amm-2017-0124>
- [38] C.I. Tarcea, C.M. Pantilimon, G. Coman, A.A. Turcanu, A.M. Predescu, E. Matei, A.C. Berbecaru, C. Predescu, Photocatalytic TiO₂ Nanostructures Developed on the Grade 2 Ti Material. *Arch. Metall. Mater.* **67** (3), 1079-1084 (2022). DOI: <https://doi.org/10.24425/amm.2022.139706>
- [39] J.C. Sin, C.A. Lim, S.M. Lam, A.R. Mohamed, H. Zeng, Facile Synthesis of Novel ZnO/Nd-doped BiOBr Composites with Boosted Visible Light Photocatalytic Degradation of Phenol. *Mater. Lett.* **248**, 20-23 (2019). DOI: <https://doi.org/10.1016/j.matlet.2019.03.129>